Mechanical Model of Neural Tissue Displacement During Lorentz Effect Imaging

Bradley J. Roth[1*] and Peter J. Basser[2]

Allen Song and coworkers recently proposed a method for MRI detection of biocurrents in nerves called "Lorentz effect imaging." When exposed to a magnetic field, neural currents are subjected to a Lorentz force that moves the nerve. If the displacement is large enough, an artifact is predicted in the MR signal. In this work, the displacement of a nerve of radius a in a surrounding tissue of radius b and shear modulus μ is analyzed. The nerve carries a current density J and lies in a magnetic field B. The solution to the resulting elasticity problem indicates that the nerve moves a distance $\frac{BJ}{4\mu}a^2 ln\left(\frac{b}{a}\right)$. Using realistic parameters for a human median nerve in a 4T field, this calculated displacement is 0.013 μm or less. The distribution of displacement is widespread throughout the tissue, and is not localized near the nerve. This displacement is orders of magnitude too small to be detected by conventional MRI methods. Magn Reson Med 61:59–64, 2009. © 2008 Wiley-Liss, Inc.

Key words: magnetic resonance imaging; MRI; Lorentz force; elasticity; displacement; action current

In recent years, many researchers have attempted to detect currents (1–5), including neural currents (6–8), by magnetic resonance imaging (MRI). This technique differs from functional MRI using the blood oxygenation level-dependent (BOLD) signal (9). With BOLD, changes in the metabolic activity of neurons is presumed to change blood oxygenation, which in turn changes the magnetic susceptibility of the blood, thereby modifying the magnetic field and influencing the MR signal. With direct detection of neuronal currents, the biocurrent itself produces a local magnetic field perturbation that contributes to the gradient field used to produce the image. Bandettini et al. (10) have reviewed this research, asking whether direct detection of neuronal current with MRI is "fantasy, possibility, or reality."

Allen Song and coworkers (11–14) recently proposed an alternative method for MRI detection of biocurrents, called "Lorentz effect imaging." When exposed to a magnetic field, biocurrents are subjected to a Lorentz force that deforms the tissue, causing the current-carrying nerve fibers to move. If a magnetic field gradient is also present, this displacement causes the spins to dephase, resulting in an artifact in the MR signal. Song and Takahashi (11) demonstrated this method by imaging the movement of a copper wire in a gel phantom using MRI. More recently, Truong and Song (13) performed an experiment on a human median nerve, applying "a series of oscillating gradients (with positive and negative lobes of the same amplitude and duration) in synchrony with the neural stimulation, such that the neuroelectric activity occurs only during the negative lobes." They concluded that "the successful detection of neuroelectric activity in vivo by using our technique demonstrates that neural activation can be imaged noninvasively by MRI with a high spatial and temporal resolution." Basford et al. (15) have also examined Lorentz-force-induced motion during MRI.

In this work, our goal is to estimate the displacement of a nerve carrying an action current, which is immersed in a static magnetic field. We solve the resulting elasticity problem including the Lorentz force as a body force, and use this result to analyze Truong and Song's (13) experiment to detect neural activation using MRI.

MATERIALS AND METHODS

Consider a cylindrical nerve of radius a lying at the center of a conducting cylinder of radius b, like the median nerve in the arm (Fig. 1). The nerve carries an intracellular current density J uniformly distributed over its cross section. An equal current returns in the extracellular space, but the extracellular current density is smaller because of the larger cross-sectional area. A uniform, steady magnetic field B is directed perpendicular to the nerve.

In our mechanical model the tissue is subject to three forces. The first two are similar to those in the fluid-fiber-collagen model of cardiac muscle (16): a pressure caused by the incompressible fluid, and a shear force characterized by the tissue shear modulus, μ. The third is the Lorentz force acting on a current in a magnetic field.

We calculate the displacement of the tissue using the Maxwell stress tensor from electrodynamics (17) and Navier's equation from the theory of elasticity (18). The derivation, which is quite mathematical, is given in the Appendix.

RESULTS

Figure 2 shows the displacement produced by the Lorentz force, calculated from Eqs. [5], [10], and [12] in the Appendix. The left panel (Fig. 2a) plots the displacement over the entire tissue ($b = 25a$, with the outer circle indicating b and the inner circle a), and the right panel (Fig. 2b) shows more detail in the region near the nerve. The displacement is continuous across the nerve boundary, and the displacement arrows form closed loops (as they must,

[1]Department of Physics, Oakland University, Rochester, Michigan, USA.

[2]Section on Tissue Biophysics and Biomimetics, Eunice Kennedy Shriver National Institute of Child Health and Human Development, National Institutes of Health, Bethesda, Maryland, USA.

Grant sponsor: National Institutes of Health (NIH); Grant number: R01EB008421; Grant sponsor: Intramural Research Program of the Eunice Kennedy Shriver National Institute of Child Health and Human Development, NIH.

*Correspondence to: Bradley J. Roth, Dept. of Physics, Oakland University, Rochester, MI 48309. E-mail: roth@oakland.edu.

Received 12 November 2007; revised 25 June 2008; accepted 7 July 2008.

DOI 10.1002/mrm.21772

Published online in Wiley InterScience (www.interscience.wiley.com).

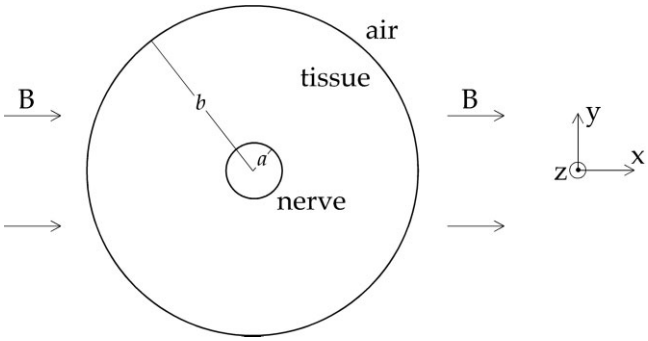

FIG. 1. A nerve of radius a lying in surrounding tissue of radius b. The magnetic field B is in the x direction. Current inside the nerve flows in the positive z direction (out of the page), and current in the surrounding tissue flows in the negative z direction. The Lorentz force on the nerve is in the y direction, consistent with the "right-hand rule."

since the tissue is incompressible). The displacement is not well localized to the region around the nerve, but spreads throughout the entire tissue, implying that the spins are dephased throughout the arm, not just near the nerve. Localizing the nerve within an MR image volume would therefore be difficult.

The most important result derived in the Appendix is that the center of the nerve is displaced by a distance $\frac{BJ}{4\mu}a^2 ln\left(\frac{b}{a}\right)$. We can estimate the magnitude of this displacement using realistic values for the parameters. In the MRI scanner used by Truong and Song (13), the magnetic field is $B = 4$ T. The shear modulus of soft tissue is approximately $\mu = 10^4$ Pa (16). We assume that the entire human median nerve is simultaneously active, and set $a = 2$ mm (19). In addition, we let $b = 25a$, which is on the order of the size of the human arm and should ensure that the assumption of $b \gg a$ is satisfied. The current density can be estimated by assuming a conductivity of 1 S/m and an electric field corresponding to the amplitude of the action potential (100 mV) over a distance of 10 mm, resulting in $J = 10$ A/m^2. The resulting displacement is 0.013 μm. This result is sensitive to the nerve radius because of the factor of a^2. If we model a single active axon with radius 10 μm, the displacement is only 1 pm.

To be conservative, in the preceding paragraph we assigned values to uncertain parameters that would magnify the Lorentz force effect. We assumed that the entire nerve was active simultaneously. During Truong and Song's (13) experiment, all the axons in the median nerve were not active because they stimulated below the motor threshold, and therefore they did not excite any of the motor axons and only the larger of the sensory axons. Our values for the conductivity of the intracellular space, the electric field in an axon, and the radius of the nerve are reasonable but probably somewhat high. The calculation is not very sensitive to the radius of the arm, but that value was also overestimated for all but the largest arms. Given these limitations, the value of 0.013 μm should be considered an upper limit for the displacement.

DISCUSSION

Our calculated displacement is too small and diffuse to explain the data obtained by Truong and Song (13). What, then, is the explanation? We do not have a satisfactory answer to this question. They performed several controls in their experiment, such as delaying the electrical stimulation of the nerve by 50 ms so it was not in sync with their magnetic field gradients, and the signal disappeared as they expected. They were careful to avoid any direct muscle excitation, and performed controls to rule out artifacts caused by eddy currents induced by the rapidly changing magnetic field gradients. These controls support their hypothesis that the measured signal is related to nerve conduction.

How can we reconcile Truong and Song's (13) observations with our calculation? We can think of four potential problems with the experiment. First, perhaps they excited a few skeletal muscle fibers—too few to produce a signal in the electromyogram or visible contraction of the muscle, but enough to cause minute displacements. Second, their data may be influenced by the magnetic field of the nerve action potential itself (6–8). For the parameters in our calculation, the magnetic field at the nerve surface is about 1.3×10^{-8} T (20), compared to the product of the magnetic field gradient used by Truong and Song (13) ($G = 36$ mT/m) and our predicted displacement ($u_y = 0.013$ μm), $Gu_y = 5 \times 10^{-10}$ T. Therefore, the magnetic field produced by the axon itself should have a more than 25 times greater influence on the signal than the Lorentz displacement. However, during their control experiment the signal disappeared when no gradient was applied, suggesting the magnetic field itself is not the primary source of the signal. Third, Lorentz force imaging and diffusion imaging use similar pulse sequences and magnetic field gradients (21). Changes in diffusion associated with nerve activation may be masquerading as a Lorentz force signal. Fourth, their displacement may be small but their technique may be sensitive to submicron displacements. Denk et al. (22) measured oscillatory flow in the cochlea using an MRI technique similar to that used by Truong and Song (13). They estimated that the minimum displacement they could detect would be about 0.16 μm, using an imaging

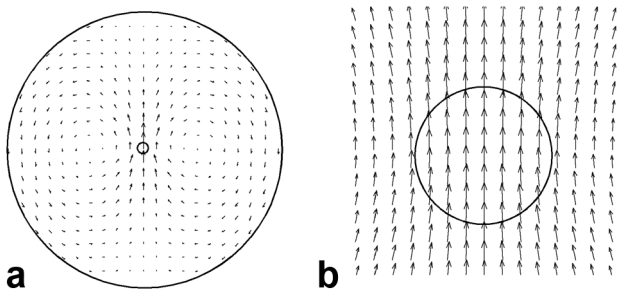

FIG. 2. The displacement produced by the Lorentz force, calculated using Eqs. [5], [10], and [12]. **a:** The entire tissue. The outer circle has radius b and the inner circle radius a ($b = 25a$). **b:** A detailed view of the displacement around the nerve. In the figure, the arrow length is exaggerated compared to the predicted displacement. The scale for the length of the arrows is set by the displacement at the center of the nerve (Eq. [22]).

system with large gradients (470 mT/m) to produce high spatial resolution images of rats. We predict that the displacement in Truong and Song's (13) experiment was smaller than the minimum that Denk et al. could detect, and it was measured using weaker gradients (36 mT/m). Put another way, the phase shift induced during Truong and Song's (13) experiment by our predicted displacement u_y is on the order of $\gamma G u_y \delta = 0.00063$ rad $= 0.036°$, where γ is the gyromagnetic ratio of a proton (2.7×10^8 s^{-1} T^{-1}), and δ is the duration of the gradient pulse (5 ms) (13). Truong and Song (13) used three cycles of oscillating gradients, so their phase shift may have been three times as large, or about 0.1°. We are skeptical that they could detect such small phase shifts.

Perhaps the small size of the predicted displacement arises because of a problem with our model. What are some of the limitations of this calculation? The calculation is based on the following assumptions:

- The current density J is uniform along the nerve, independent of z. In a real nerve, J does vary with z. For a large myelinated axon, the speed of propagation can be as high as 100 m/s, and the upstroke of the action potential lasts about 0.5 ms, implying that the current associated with the action potential upstroke is spread over a length of 50 mm. This length is larger than a nerve radius, and much larger than an axon radius, but may be similar to the radius of the surrounding tissue, such as the arm surrounding the median nerve. Smaller axons have slower speeds, so this length could be shorter in slower axons (an estimate of 10 mm was used in our calculation of J). We make this assumption in part because accounting for variation in the current in the z direction would make an analytical solution difficult, necessitating numerical methods (23,24). Moreover, the depolarization and repolarization phases of the action potential produce intracellular currents in opposite directions at different locations along the axon, reducing the net Lorentz force and resulting in smaller displacements. Finally, different axons have different conduction velocities, so the relative position and timing of the upstroke in each axon varies as their action potentials propagate, further reducing the net displacement. Thus, relaxing our assumption of a uniform current would generally make the displacement smaller.
- The intracellular current density is uniform across the cross section of the nerve, independent of r. Calculation of the intracellular potential and current associated with a propagating action potential along a nerve axon indicates that the axial current density should be nearly uniform across the axon cross section (24). In this macroscopic model, we assume the active axons are uniformly distributed throughout the nerve cross section.
- The extracellular current density is distributed uniformly throughout the extracellular space. The validity of this assumption should improve as the spatial extent of the action potential upstroke increases. In the limit of a uniform current along the axon, we expect the extracellular current to distribute uniformly, so this assumption is related to our first assumption of a uniform intracellular current along the axon. For a current that is localized along the axon, the extracellular current will be greater near the axon than far from it (23,24). In general, extracellular currents spread out radially over a distance comparable to the axial extent of the action potential (estimated at 50 mm above). If we relax this assumption, the forces on the intracellular and extracellular currents would probably cancel more completely (as in a coaxial cable), implying a smaller displacement (although perhaps a more localized distribution).
- A steady-state elastic model. This assumption ignores phenomena associated with the propagation of acoustic waves and therefore provides accurate results when the acoustic wavelength is much greater than the other dimensions in the problem. The wavelength of a sound wave in tissue is large (about 1.5 m) at the 1 kHz frequency characteristic of a nerve action potential. Therefore, the steady-state model should be accurate.
- The nerve and surrounding tissue are homogeneous and isotropic. Both the electrical and mechanical properties are heterogeneous in real tissue, and both neural and muscle tissue are anisotropic, but properly accounting for heterogeneity and anisotropy would require a much more elaborate numerical model than the one we derive here. Our results represent an initial approximation, which may need to be refined and extended in later work.
- Viscoelastic and poroelastic material behaviors are ignored. For the assumed rapid change in current (a few milliseconds), one can neglect viscoelastic or poroelastic effects. At short times, the material could be assumed to be incompressible. For tissue that is poroelastic, there is insufficient time for the fluid phase to flow through the solid or network phase (25). Similar arguments can be applied for viscoelastic models of tissues with dashpot elements. Generally, including either of these two dissipative mechanisms would tend to reduce the net displacement of the tissue, so using a linearly elastic model of the tissue will always result in larger net displacements. Including these effects in the constitutive law of the tissue will only reduce the contribution of the Lorentz force to the MR image.
- A linear approximation for the strain tensor. Given the small strains predicted by this calculation, a linear approximation for the strain should be very accurate.
- The nerve is located at the center of the arm. Results might vary if the nerve is off-center. However, either a numerical model or a much more complicated analytical model would be required to treat an off-center nerve (23). Moreover, we see no reason why a nonconcentric nerve should magnify the displacement significantly.
- The tissue shear modulus is 10,000 Pa. Our value is on the order of the shear modulus for many soft tissues (16,25,26), but might not be accurate for the skeletal muscle surrounding a human median nerve. One advantage of an analytical model is that it highlights which parameters are important in a problem. The shear modulus is crucial for determining the magni-

tude of the displacement, but is not typically measured in experiments. Our results suggest that the magnitude of the displacement is inversely proportional to the shear modulus, but the spatial distribution is independent of it. So, our conclusions about the distribution of displacement should hold regardless of the shear modulus value.

- The nerve is elastically coupled to the surrounding tissue. One key question regarding our mechanical model is: How well attached is the nerve to the tissue around it? If the nerve could somehow slide through the tissue without exerting any stress on its surroundings, our model would provide an erroneous view of the displacement distribution. We find it difficult to imagine how this would be possible.
- The outer boundary is free. We have solved the same problem with a fixed outer boundary instead of a free one. Although the displacement distribution is somewhat different in this case, the magnitude of the displacement at the center of the nerve is the same.
- The effect of myelination is ignored. Most large axons in a human nerve are myelinated, which our model does not take into account. However, as estimated above, the region of depolarization of the action potential can be up to 50 mm in length, which is much greater than the distance between the nodes of Ranvier (about 1 mm). Therefore, we expect that myelination will cause only a small change in the resulting current distribution compared to an equivalent homogeneous axon (27).
- The Lorentz force acts macroscopically. We treat the Lorentz force as acting on a continuous current rather than on individual ions, in the tradition of the cable model (28). Microscopically, the Lorentz force acts on the ions themselves, but this force is transmitted to the nerve by friction within the conductor, just as the magnetic force on individual electrons results in a macroscopic force on a current-carrying wire. Truong et al. (14) considered a microscopic model and concluded that "ionic currents with durations and current densities on the same order of magnitude as those induced by neuroelectric activity in nerve fibers and in the brain can be detected [by MRI]." However, they assumed a frictional force consistent with a mobility of 0.13 (m/s)/(V/m). The measured mobilities of ions important in nerve conduction are on the order of 7×10^{-8} (m/s)/(V/m) (29). Thus, they may have overestimated the Lorentz force by a factor of more than 1 million.
- Incoherent intravoxel phase shifts. Song and Takahashi (11) have suggested that the Lorentz effect signal arises from "intravoxel incoherent phase shifts." The only way intravoxel dephasing could account for a signal larger than the one we predict is if microscopic incoherent displacements were much larger than the macroscopic coherent displacement that we calculate. We do not know what mechanism would produce such large microscopic displacements.

CONCLUSIONS

In conclusion, we use the theories of electromagnetism and elasticity to predict the displacement ascribed to the Lorentz force in the experiment by Truong and Song (13), and find that it is less than 0.013 μm. A displacement this small would probably not be detectable using their experimental technique. Thus, we suspect that some other effect besides a Lorentz force-induced displacement is responsible for their measured signal.

ACKNOWLEDGMENT

We thank Liz Salak for editing the manuscript. Supported by the Intramural Research Program of the Eunice Kennedy Shriver National Institute of Child Health and Human Development, National Institutes of Health (NIH) (to P.J.B.) and NIH grant R01EB008421 (to B.J.R.).

APPENDIX

Consider a cylindrical nerve of radius a lying at the center of a conducting cylinder of radius b (Fig. 1). Position is described by a cylindrical coordinate system (r, θ, z), and the problem is assumed to be independent of z. The nerve carries a current density J uniformly distributed over its cross section. An equal current returns in the extracellular space, but because of the different cross-sectional areas the extracellular current density is $j = J\frac{a^2}{b^2 - a^2}$, where the minus sign indicates that the intracellular and extracellular currents flow in the opposite directions. A uniform, steady magnetic field B is in the x-direction.

In our mechanical model the tissue experiences pressure and undergoes displacements. The stress tensor, τ_{ij}, is

$$\tau_{ij} = -p\delta_{ij} + 2\mu\varepsilon_{ij} + T_{ij}, \qquad [1]$$

where p is the hydrostatic fluid pressure, ε_{ij} is the strain tensor, μ is the tissue shear modulus, and T_{ij} is the Maxwell stress tensor that results in the Lorentz force $\boldsymbol{F}=\boldsymbol{J}\times\boldsymbol{B}$. The first two terms of this stress tensor are similar to those in the fluid-fiber-collagen model derived by Ohayon and Chadwick (16) to describe the mechanical properties of cardiac muscle. Equation [1] does not include any viscoelastic or poroelastic behavior.

The stress tensor specifies that state of internal stress in the tissue, but in order to determine the net force on the tissue we must examine spatial derivatives of the stress tensor. The divergence of Eq. [1] gives Navier's equation that describes the elastic state of the medium in static equilibrium (steady-state), and says that the sum of the forces (elastic plus magnetic) is zero. Navier's equation in polar coordinates is (18)

$$-\frac{\partial p}{\partial r} + 2\mu\left(\frac{\partial \varepsilon_{rr}}{\partial r} + \frac{1}{r}\frac{\partial \varepsilon_{r\theta}}{\partial \theta} + \frac{\varepsilon_{rr} - \varepsilon_{\theta\theta}}{r}\right) + F_r = 0, \qquad [2]$$

$$-\frac{1}{r}\frac{\partial p}{\partial \theta} + 2\mu\left(\frac{\partial \varepsilon_{r\theta}}{\partial r} + \frac{1}{r}\frac{\partial \varepsilon_{\theta\theta}}{\partial \theta} + \frac{2\varepsilon_{r\theta}}{r}\right) + F_\theta = 0. \qquad [3]$$

In the linear approximation, the displacement of the tissue, $\boldsymbol{u} = (u_r, u_\theta)$, is related to the strain tensor by (18)

$$\varepsilon_{rr} = \frac{\partial u_r}{\partial r};\ \varepsilon_{\theta\theta} = \frac{u_r}{r} + \frac{1}{r}\frac{\partial u_\theta}{\partial \theta};\ \varepsilon_{r\theta} = \frac{1}{2}\left(\frac{1}{r}\frac{\partial u_r}{\partial \theta} + \frac{\partial u_\theta}{\partial r} - \frac{u_\theta}{r}\right). \quad [4]$$

We assume that the tissue is incompressible ($\nabla \cdot \boldsymbol{u} = 0$), which implies that the displacement can be specified by a stream function ψ, a scalar function whose spatial derivatives give the radial and azimuthal components of the displacement vector (18)

$$u_r = -\frac{1}{r}\frac{\partial \psi}{\partial \theta};\ u_\theta = \frac{\partial \psi}{\partial r}. \quad [5]$$

These relationships allow the solution of Navier's equation to be stated in terms of two scalar functions: the pressure and the stream function. The uniqueness of these solutions will depend on the boundary conditions (30).

The Maxwell stress tensor T_{ij} inside the nerve ($r < a$) is (17)

$$T_{rr} = \frac{BJ}{2} r\, sin\theta,\ T_{\theta\theta} = -\frac{BJ}{2} r\, sin\theta, \text{ and } T_{r\theta} = \frac{BJ}{2} r\, cos\theta. \quad [6]$$

The divergence of T_{ij} is simply the body force per unit volume $\boldsymbol{F}=\boldsymbol{J}\times\boldsymbol{B}$, which for this geometry is

$$F_r = BJ\, sin\theta,\ F_\theta = BJ\, cos\theta. \quad [7]$$

In Cartesian coordinates, this is simply a force per unit volume of magnitude BJ in the y-direction, consistent with the "right-hand rule." Outside the nerve ($a < r < b$), the form of T_{ij} is more complicated:

$$T_{rr} = \frac{BJ}{2} sin\theta\left[\frac{a^2}{r} - \frac{a^2}{b^2 - a^2}\left(r - \frac{a^2}{r}\right)\right],$$

$$T_{\theta\theta} = -\frac{BJ}{2} sin\theta\left[\frac{a^2}{r} - \frac{a^2}{b^2 - a^2}\left(r - \frac{a^2}{r}\right)\right],$$

and

$$T_{r\theta} = \frac{BJ}{2} cos\theta\left[\frac{a^2}{r} - \frac{a^2}{b^2 - a^2}\left(r - \frac{a^2}{r}\right)\right], \quad [8]$$

but the Lorentz force is given simply by

$$F_r = -BJ\frac{a^2}{b^2 - a^2}\, sin\theta,\ F_\theta = -BJ\frac{a^2}{b^2 - a^2}\, cos\theta, \quad [9]$$

which is equal to a force Bj in the negative y direction.

At the boundary of the nerve ($r = a$), the displacement (u_r and u_θ) and the components of the stress tensor (τ_{rr} and $\tau_{r\theta}$) are assumed to be continuous. At the outer boundary ($r = b$) the surface is "stress-free" ($\tau_{rr} = \tau_{r\theta} = 0$).

We have found an analytical solution to Navier's equation subject to these boundary conditions. Inside (i) and outside (e) of the nerve, the stream function and pressure are given by

$$\psi_i = \frac{BJ}{4\mu} a^3 cos\theta\left[-\frac{1}{4}\left(1 + \left(\frac{a}{b}\right)^2\right)\left(\frac{r}{a}\right)^3 + \left(\frac{r}{a}\right) ln\left(\frac{b}{a}\right)\right], \quad [10]$$

$$p_i = \frac{BJ}{2} a\left(1 - \left(\frac{a}{b}\right)^2\right)\left(\frac{r}{a}\right) sin\theta, \quad [11]$$

$$\psi_e = \frac{BJ}{4\mu} a^3 \left(\frac{1}{1 - \left(\frac{a}{b}\right)^2}\right) cos\theta\left[\frac{1}{4}\left(\left(\frac{a}{b}\right)^4\left(\frac{r}{a}\right)^3 - \left(\frac{a}{r}\right)\right) + \left(\frac{r}{a}\right) \times \left(ln\left(\frac{b}{r}\right) - \left(\frac{a}{b}\right)^2 ln\left(\frac{b}{a}\right)\right)\right], \quad [12]$$

$$p_e = \frac{BJ}{2} a\left(\frac{1}{1 - \left(\frac{a}{b}\right)^2}\right) sin\theta\left[-\left(\frac{a}{b}\right)^2\left(2 - \left(\frac{a}{b}\right)^2\right)\left(\frac{r}{a}\right) + \left(\frac{a}{r}\right)\right]. \quad [13]$$

These expressions are complicated, but become simpler if $b \gg a$. This means that the return path has a significantly larger area than the nerve carrying the action current.

$$\psi_i = \frac{BJ}{4\mu} a^3 cos\theta\left[-\frac{1}{4}\left(\frac{r}{a}\right)^3 + \left(\frac{r}{a}\right) ln\left(\frac{b}{a}\right)\right], \quad [14]$$

$$p_i = \frac{BJ}{2} a\left(\frac{r}{a}\right) sin\theta, \quad [15]$$

$$\psi_e = \frac{BJ}{4\mu} a^3 cos\theta\left[-\frac{1}{4}\left(\frac{a}{r}\right) + \left(\frac{r}{a}\right) ln\left(\frac{b}{r}\right)\right], \quad [16]$$

$$p_e = \frac{BJ}{2} a\left(\frac{a}{r}\right) sin\theta. \quad [17]$$

Note that b cannot be removed entirely from these expressions even if it is much larger than a; it still appears as an argument of the logarithm in the stream function.

For the case of $b \gg a$, the displacement inside the nerve is

$$u_r = \frac{BJ}{4\mu} a^2 sin\theta\left[-\frac{1}{4}\left(\frac{r}{a}\right)^2 + ln\left(\frac{b}{a}\right)\right], \quad [18]$$

$$u_\theta = \frac{BJ}{4\mu} a^2 cos\theta\left[-\frac{3}{4}\left(\frac{r}{a}\right)^2 + ln\left(\frac{b}{a}\right)\right], \quad [19]$$

and outside the nerve is

$$u_r = \frac{BJ}{4\mu} a^2 sin\theta\left[-\frac{1}{4}\left(\frac{a}{r}\right)^2 + ln\left(\frac{b}{a}\right)\right], \quad [20]$$

$$u_\theta = \frac{BJ}{4\mu} a^2 cos\theta\left[\frac{1}{4}\left(\frac{a}{r}\right)^2 - 1 + ln\left(\frac{b}{a}\right) - ln\left(\frac{r}{a}\right)\right]. \quad [21]$$

The center of the nerve is displaced by $u_r = \frac{BJ}{4\mu}a^2 ln\left(\frac{b}{a}\right) sin\theta$ and $u_\theta = \frac{BJ}{4\mu}a^2 ln\left(\frac{b}{a}\right) cos\theta$, or simply

$$u_y = \frac{BJ}{4\mu}a^2 ln\left(\frac{b}{a}\right). \quad [22]$$

REFERENCES

1. Joy M, Scott G, Henkelman M. In vivo detection of applied electric currents by magnetic resonance imaging. Magn Reson Imaging 1989;7: 89–94.
2. Bodurka J, Jesmanowicz A, Hyde JS, Xu H, Estkowski L, Li S-J. Current-induced magnetic resonance phase imaging. J Magn Reson 1999;137: 265–271.
3. Scott GC, Joy MLG, Armstrong RL, Henkelman RM. Measurement of nonuniform current density by magnetic resonance. IEEE Trans Med Imaging 1991;10:362–374.
4. Scott GC, Joy MLG, Armstrong RL, Henkelman RM. Sensitivity of magnetic-resonance current-density imaging. J Magn Reson 1992;97: 235–254.
5. Joy MLG, Lebedev VP, Gati J. Imaging of current density and current pathways in rabbit brain during transcranial electrostimulation, IEEE Trans Biomed Eng 1999;46:1139–1149.
6. Singh M. Sensitivity of MR phase-shift to detect evoked neuromagnetic fields inside the head. IEEE Trans Nucl Sci 1994;41:349–351.
7. Kamei H, Iramina K, Yoshikawa K, Ueno S. Neuronal current distribution imaging using magnetic resonance. IEEE Trans Magn 1999;35: 4109–4111.
8. Bodurka J, Bandettini PA. Toward direct mapping of neural activity: MRI detection of ultraweak, transient magnetic field changes. Magn Reson Med 2002;47:1052–1058.
9. Ogawa S, Lee TM, Kay AR, Tank DW. Brain magnetic resonance imaging with contrast dependent on blood oxygenation. Proc Natl Acad Sci USA 1990;87:9868–9872.
10. Bandettini PA, Petridou N, Bodurka J. Direct detection of neuronal activity with MRI: fantasy, possibility, or reality? Appl Magn Reson 2005;29:65–88.
11. Song AW, Takahashi AM. Lorentz effect imaging. Magn Reson Imaging 2001;19:763–767.
12. Truong T-K, Wilbur JL, Song AW. Synchronized detection of minute electrical currents with MRI using Lorentz effect imaging. J Magn Reson 2006;179:85–91.
13. Truong T-K, Song AW. Finding neuroelectric activity under magnetic-field oscillations (NAMO) with magnetic resonance imaging in vivo. Proc Natl Acad Sci USA 2006;103:12598–12601.
14. Truong T-K, Avram A, Song AW. Lorentz effect imaging of ionic currents in solution. J Magn Reson 2008;191:93–99.
15. Basford AT, Basford JR, Kugel J, Ehman RL. Lorentz-force-induced motion in conductive media. Magn Reson Imaging 2005;23:647–651.
16. Ohayon J, Chadwick RS. Effects of collagen microstructure on the mechanics of the left ventricle. Biophys J 1988;54:1077–1088.
17. Jackson JD. Classical electrodynamics. 3rd ed. New York: Wiley; 1999.
18. Love AEH. A treatise on the mathematical theory of elasticity. New York: Dover; 1944.
19. Hammer HB, Hovden IAH, Haavardsholm EA, Kvien TK. Ultrasonography shows increased cross-sectional area of the median nerve in patients with arthritis and carpal tunnel syndrome. Rheumatology 2006;45:584–588.
20. Roth BJ, Wikswo Jr JP. The magnetic field of a single axon: a comparison of theory and experiment. Biophys J 1985;48:93–109.
21. Li T, Song AW. Fast functional brain signal changes detected by diffusion weighted fMRI. Magn Reson Imaging 2003;21:829–833.
22. Denk W, Keolian RM, Ogawa S, Jelinski LW. Oscillatory flow in the cochlea visualized by a magnetic resonance imaging technique. Proc Natl Acad Sci USA 1993;90:1595–1598.
23. Clark J, Plonsey R. The extracellular potential field of the single active nerve fiber in a volume conductor. Biophys J 1968;8:842–864.
24. Woosley JK, Roth BJ, Wikswo Jr JP. The magnetic field of a single axon: a volume conductor model. Math Biosci 1985;76:1–36.
25. Basser PJ. Interstitial pressure, volume, and flow during infusion into brain tissue. Microvasc Res 1992;44:143–165.
26. Dresner MA, Rose GH, Rossman PJ, Muthupillai R, Manduca A, Ehman RL. Magnetic resonance elastography of skeletal muscle. J Magn Reson Imaging 2001;13:269–276.
27. Basser PJ. Cable equation for a myelinated axon derived from its microstructure. Med Biol Eng Comput 1993;31:S87–S92.
28. Roth BJ, Basser PJ. A model of the stimulation of a nerve fiber by electromagnetic induction. IEEE Trans Biomed Eng 1990;37:588–597.
29. Katz B. Nerve, muscle, and synapse. New York: McGraw Hill; 1966.
30. Aldroubi A, Chadwick RS. On the uniqueness of quasi-static solutions of some linear models of left ventricular mechanics. Math Biosci 1990; 99:195–203.